USING ALE-FEM TO SIMULATE THE INSTABILITY OF BEAM-TYPE NANO-ACTUATOR IN THE PRESENCE OF ELECTROSTATIC FIELD AND DISPERSION FORCES[*]

Y. TADI BENI[1], A. R. VAHDATI[2] AND M. ABADYAN[3**]

[1]Faculty of Engineering, Shahrekord University, Shahrekord, I. R. of Iran
[2]Mechanical Engineering Group, Naein Branch, Islamic Azad University, Naein, I. R. of Iran
[3]Shahrekord Branch, Islamic Azad University, Shahrekord, I. R. of Iran
Email: Abadyan@yahoo.com

Abstract– The ability of mesh design in arbitrary Lagrangian-Eulerian finite element method (ALE-FEM) makes it a generally efficient device for simulating engineering problems. In this paper, ALE-FEM is used to model the static deflection and instability of beam-type cantilever nano-actuators using plain element. Effects of electrostatic fields are taken into account through first-order fringing field corrected model. In addition, the influence of quantum vacuum fluctuations is considered via attractive Casimir and van der Waals force depending on the range of application. The instability parameters, i.e. pull-in voltage and deflection of the nano-actuator are computed. The obtained results are compared with those reported in literature using numerical method as well as Lagrangian FEM. The findings indicate that ALE method can be used as a powerful technique for modeling beam type nano-actuator.

1. INTRODUCTION

Finite element (FE) method has been applied as a powerful tool to simulate engineering problems in recent decades. The FE approach can be divided into two main branches, i.e. the Lagrangian and the Eulerian approach [1]. In the Lagrangian approach, the nodes and material points move together simultaneously and therefore this method is suitable for solid mechanics simulations. In the Eulerian approach, the meshes are fixed in space and the material points move during deformation, hence it is suitable in fluid mechanics applications. In recent years, a more general approach called Arbitrary Lagrangian-Eulerian method (ALE) has been developed which contains the advantages of both Lagrangian and Eulerian approaches, while avoiding their shortcomings [2-6]. In an ALE analysis, the FE mesh is neither attached to the material nor necessarily fixed in space, and the mesh and material point can move separately. The ability of mesh motion in ALE reduces the mesh distortion and transfers the mesh to regions which need higher mesh density without increasing the number of elements.

With the huge growth of nanotechnology in recent decades, researchers have focused on modeling the behavior of nano-actuators. A typical beam-type nano-actuator is constructed from a conductive movable cantilever electrode which is suspended over a conductive fixed ground electrode. Applying voltage difference between these electrodes causes the movable electrode to deflect towards the ground one, due to electrostatic attraction. The pull-in instability occurs when the electrostatic attraction exceeds

the elastic restoring moment of the movable electrode and leads to contact between the two electrodes. Various finite element methods are applied to simulate the pull-in instability of micro-structures [7-11]. The pull-in instability occurs when external forces (which rise from electrostatic attraction, quantum fields, etc.) exceed the elastic resistance of the micro-structure. Batra et al. [9] has used FE method to investigate the snap-through instability of micro-switches. The pull-in instability of multi-layer micro-beams has been simulated in Ref. [7] using FE approach. In nano-distances, electromagnetic quantum vacuum fluctuations between the electrodes significantly affect the instability performance of the nano-actuators as well as electrostatic Coulomb force. The effect of vacuum fluctuations can be modeled through the dispersion forces, i.e. Casimir and van der Waals attractions [12]. Useful information about the nature of quantum vacuum fluctuations in nanostructures can be found in Refs. [13, 14]. Several semi-analytical approaches, i.e. lumped parameter [15, 16], homotopy perturbation [17,18], modified Adomian decomposition [19], reduced order method [20,21], etc. have been developed to examine the instability of nano-actuators incorporating the effects of electrostatic attraction and dispersion forces. However, to the best knowledge of the authors, only a few researchers have applied FE models to investigate pull-in instability of nano-structures in the presence of both Coulomb and dispersion forces [22]. Moghimi et al. [22] has applied FEM to simulate the influence of dispersion forces on the dynamic pull-in behavior of beam-type nano-switches.

In this study, ALE-FEM method is introduced to demonstrate the effects of Casimir and van der Waals attractions on the pull-in behavior of beam-type nano-actuators using plain element. To the best of our knowledge, using plain-element for FE modeling of dispersion force in NEMS has not been addressed previously. The few FEM researches that have focused on this topic used only the beam-element [22]. The ALE-FEM results are compared with the numerical data, Lagrangian FEM as well as other results reported in the literature.

2. MODELING AND ALE FORMULATION

Figure 1 shows a 2-dimensional cantilever beam-type nano-actuator which consists of a moving electrode suspended over the conductive ground plain. The system is modeled by a beam of length L with a uniform rectangular cross section of width B and thickness H which is suspended over a conductive substrate. The initial geometry, boundary conditions and the FE model of the nano-structure are shown in this figure. The system is modeled using the proposed ALE-FEM as a plane strain problem. A feature of the ALE-FEM approach is that the density of the mesh can be varied by properly moving the mesh in the course of analysis. Therefore, it is possible to achieve higher resolution at desired locations of the mesh without increasing the number of elements. From this viewpoint, we can move the mesh in a way to have denser mesh in areas with higher stress gradients, i.e. closer to the cantilever end. This may be carried out without changing the mesh connectivity or number of elements. The initial and final mesh and the trend of its motion are shown in Fig. 1. The constitutive material of the nano-actuator is assumed linear elastic and only the static deflection of the nano-beam is considered.

The ALE finite element equation can be obtained by discretization of equation of motion similar to the previous work [3-6]. The final form of ALE equation is written as

$$ {}^t \mathbf{K}^m \mathbf{u}^{(i)} - {}^t \mathbf{K}^g \mathbf{u}^{g(i)} = \mathbf{f}^{(i)}(q) \tag{1}$$

where ${}^t \mathbf{K}^m$ and ${}^t \mathbf{K}^g$ are the element stiffness matrices related to material and grid motions, respectively and $\mathbf{f}^{(i)}$ is the element incremental load vector which contains the nonlinear form of displacement of element node. The definition of matrices ${}^t \mathbf{K}^m$ and ${}^t \mathbf{K}^g$ are given in reference [3-6].
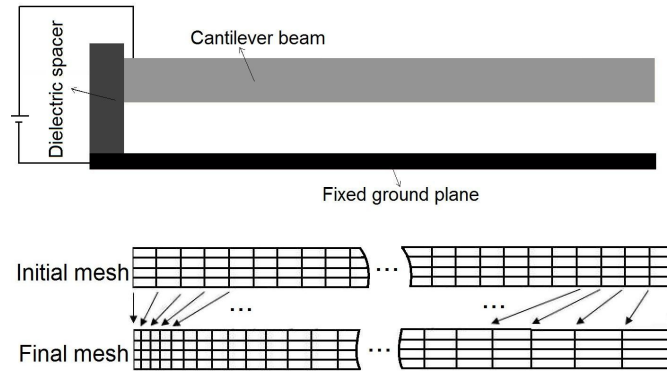
Fig. 1. Geometry, FE mesh and boundary condition for the nano beam

The distributed force along the beam is modeled as

$$q = f_{Coulomb} + f_{Dispersion}, \qquad (2)$$

where $f_{Coulomb}$ and $f_{Dispersion}$ are the electrostatic (Coulomb) and quantum (Casimir or van der Waals) forces per unit length of the beam, respectively. The electrostatic force with first order fringing correction can be presented as the following equation [23]:

$$f_{Coulomb} = \frac{\varepsilon_0 B V^2}{2(g-w)^2}\left(1 + 0.65\frac{(g-w)}{B}\right) \qquad (3)$$

where $\varepsilon_0 = 8.854 \times 10^{-12} \ C^2 N^{-1} m^{-2}$ is the permittivity of vacuum, V is the applied voltage, w is the deflection of the beam and g is the initial gap between the movable and the ground electrode.

The dispersion forces per unit length of the beam ($f_{Dispersion}$) are defined considering the van der Waals and Casimir forces. For small gap, two nano-scale interaction regimes can be defined: First, the ultra-small separation regime (typically below several ten nanometers [24]), in which the van der Waals force is the dominant attraction. In this case, the attraction between two surfaces is proportional to the inverse cube of the separation:

$$f_{Dispersion} = \frac{\bar{A}B}{6\pi(g-w)^3} \qquad (4)$$

where $\bar{A}$ is the Hamaker constant. The second regime is the large separation regime in which the Casimir force is dominant (typically above several ten nanometers [24]). Considering some idealizations, the quantum force per unit length of the actuator is [17]:

$$f_{Dispersion} = \frac{\pi^2 \mathrm{h} c B}{240(g-w)^4} \qquad (5)$$

where $\mathrm{h} = 1.055 \times 10^{-34}$ Js is Planck's constant divided by 2π and $c = 2.998 \times 108$ m/s is the light speed.

It should be noted that the value of the applied force in each node depends on the beam deflection and the position of nodes in FE mesh. Figure 2 shows a sample grid point. The applied force in each node is calculated by multiplying the force distribution (Eq. 2) by element length between two adjacent nodes and then dividing the obtained value by the nodes. The Casimir and Coulomb forces are applied to the nodes in the lower layer of the beam while van der Waals force is applied to the centerline of beam. The direct iteration method [1] is utilized to find deflections in each step. The iteration process in each step is continued until the convergence criteria of deflections are satisfactory.
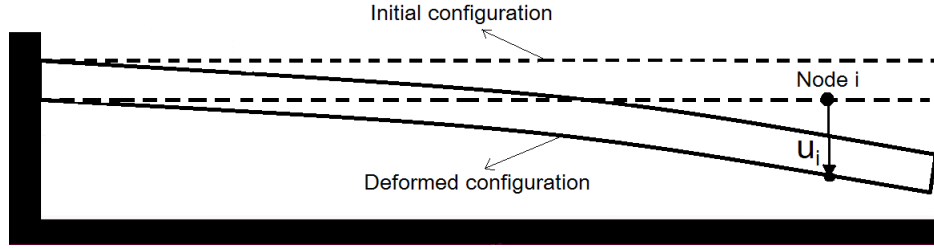
Fig. 2. Schematic view for computation method of applied forces

For a N degree of freedom system, Eq. (1) produces 2N unknowns u_i and u_i^g. Therefore, additional equations are supplied by defining a mesh motion scheme which defines the motion of grid points at the current incremental step. The supplemental equations introduce the relationship between material and grid nodal displacement [25], which is written as

$$u^{g(i)} = a + \mathbf{B} u^{(i)} \tag{6}$$

where vector a and matrix $\mathbf{B}$ are any desired motion assigned to each degree of freedom of the mesh by the mesh motion scheme [25].

By substituting Eq. (6) into Eq. (1), the unknown grid displacements are eliminated from ALE equation and only material displacement appears in the final assembled ALE equation, thus reducing the size of solution.

In this paper, the transfinite-mapping method is used for specifying grid displacements according to Ref. [25]. Final form of the equation of motion is obtained as:

$$\left({}^t\mathbf{K}^m - {}^t\mathbf{K}^g \mathbf{B} \right) u^{(i)} = \mathbf{f}^{(i)}(q) + {}^t\mathbf{K}^g a \tag{7}$$

The ALE-FE model of the total problem is found by assembling the equations of various elements. Afterwards, the fully discretized form of the total problem is obtained.

In the next section, the static pull-in behavior of the nano-actuator is investigated and obtained results are discussed. In order to compare the result of this study with those of the literature, the following dimensionless parameters, W_{tip}, α, β and γ are defined:

$$W_{tip} = \frac{w(x = L)}{g} \tag{8.1}$$

$$\alpha = \frac{\pi^2 \mathrm{h} c B L^4}{240 g^5 EI} \tag{8.2}$$

$$\eta = \frac{A B L^4}{6\pi g^4 EI} \tag{8.3}$$

$$\beta = \frac{\varepsilon_0 B V^2 L^4}{2 g^3 EI} \tag{8.4}$$

$$\gamma = 0.65 \frac{g}{B} \tag{8.5}$$

where E is Young's modulus, I is axial moment of inertia for the rectangular cross-section, B is width of rectangular cross section of beam, H is height of beam cross section and L is the length of nano-beam.

Relations (8-a), (8-b), (8-c), (10-d) and (8-e) correspond to dimensionless values of tip deflection, Casimir force, van der Waals attraction, applied voltage and fringing effect, respectively.

3. RESULTS AND DISCUSSION

a) Simulation result

In order to demonstrate the ability of the presented ALE method in investigating the instability of cantilever nano-actuators, a typical narrow nano-actuator with L=30 μm, H=1 μm, g=2.5 μm, w=g and E=70 GPa is simulated. The deformed shape and FE mesh of the nano-actuator during the deformation are depicted in Figs. 3 and 4. Figs. 3 and 4 show the deflection of the actuator considering Casimir and van der Waals regime, respectively. When β increases from zero (Figs. 3b and 4b) to the critical pull-in instability point (Figs. 3d and 4d), mesh resolution increases near the fixed end of the beam due to the increase in elastic deformation at this region.
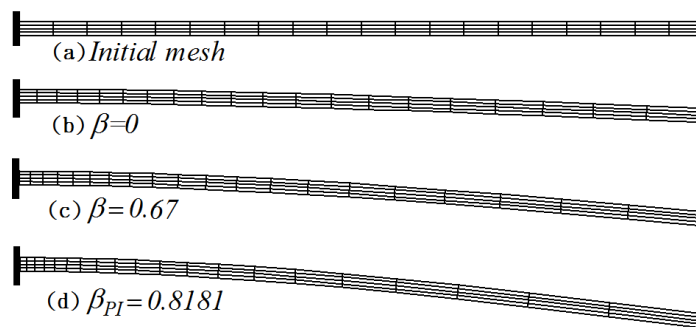

(a) *Initial mesh*

(b) β=0

(c) β= 0.67

(d) β_{PI}= 0.8181

Fig. 3. Deformed shapes and mesh motions during the deformation of actuator under Casimir force

(a) *Initial mesh*

(b) β=0

(c) β= 0.47

(d) β_{PI} = 0.6677

Fig. 4. Deformed shapes and mesh motions during the deformation of under van der Waals force

In order to guarantee the reliability of the ALE method, the convergence of the obtained results is checked and the results are reported in Table 1. The number of elements are increased in height and length directions and the grid independency analysis is conducted. For the number of elements above 80, the error in computing pull-in voltage is less than 1 %.

Table 1. Mesh convergence study result

Number of elements (horizontal × vertical)	β_{PI} *(With Casimir effect)*	β_{PI} *(With van der Waals effect)*
20(10×2)	0.7211	0.5865
40(20×2)	0.8081	0.6655
60(30×2)	0.8191	0.6681
40(10×4)	0.7333	0.5934
60(15×4)	0.7865	0.6333
80(20×4)	0.8181	0.6677
100(25×4)	0.8185	0.6680

Figure 5 shows the relationships between dimensionless applied voltage (β) and cantilever tip deflection (W_{tip}) neglecting the quantum effects. Ignoring dispersion forces is a common assumption in modeling actuators with large initial gap values. This figure reveals that the fringing field effect (increase in γ) increases the instability deflection while reducing the instability voltage of the system. It is observed that ALE-FEM results are in excellent agreement with the numerical results. Furthermore, ALE results are much closer to the numerical solution in comparison with those obtained in [17] using truncated series solution. This figure reveals that the proposed ALE technique is highly reliable to simulate the pull-in performance of nano-actuators. The ALE-FEM can be utilized as a powerful method in design procedures.
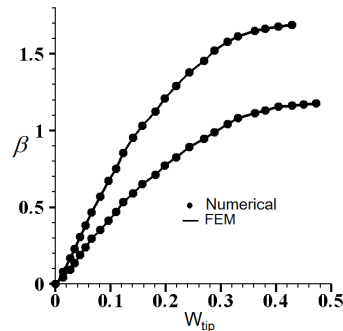
Fig. 5. Relationships between β and cantilever tip deflection with and
without fringing field effects, $\alpha = \eta = 0$

The influence of dispersion forces (α and η) on the tip deflection of the actuator (W_{tip}) for $\gamma=0.65$ is depicted in Figs. 6 and 7. These figures reveal that increase in vacuum fluctuations decreases the pull-in deflection and voltage of the actuator. Furthermore, the beam has initial deflection due to the presence of the dispersion forces even when no voltage is applied ($\beta=0$). Interestingly, when the initial gap is small enough the nano-actuator can collapse onto the ground plane due to the dispersion forces even without any voltage appliance.
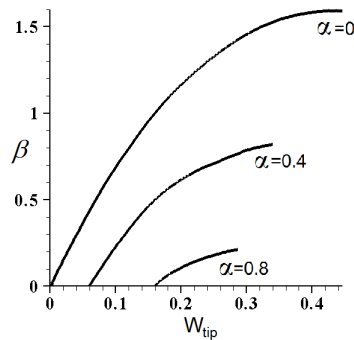
Fig. 6. Relationships between β and tip deflection of a nano-beam
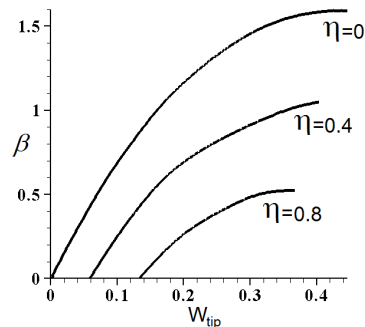for various Casimir parameters

Fig. 7. Relationships between β and tip deflection of a nano-beam
for various van der Waals parameters

b) Comparing ALE with other methods

In order to compare the ALE-FEM results with those of the literature, the critical values of dispersion forces, i.e. α_c and η_c, have been reported in Table 2. Note that when the dispersion forces between the planes are large enough, the movable beam might collapse onto the ground without applying voltage. As seen, the critical values of dispersion force predicted via ALE-FEM are very close to the numerical values. This table reveals the reliability of the ALE-FEM in simulating nano-actuators.

Table 2. Comparison of the ALE-FEM with other methods when no voltage
is applied on the actuator ($\beta=0$)

Model	α_C	Relative difference with numerical solution	η_C	Relative difference with numerical solution
Numerical Solution [17]	0.94	-	1.21	-
HPM [17]	0.81	13.8	1.20	0.8
Lumped Model [17]	0.66	29.8	0.84	30.6
Modified Adomian [19]	0.96	2.1	1.23	1.7
Present method (ALE-FEM)	0.95	1.0	1.22	0.8

It should be mentioned that the numerical solution in [17] is applied on the Euler beam theory. Therefore, this numerical solution is valid only for long beams ($l/w>10$) and is not acceptable for short actuators. However, the present ALE-FEM is reliable for both long and short beams due to application of the plane elements. Table 3 shows the comparison between numerical and ALE results for various beam length. This table reveals that the numerical and ALE results are very close for long beam but have considerable differences with numerical results in the case of short beam.

Table 3. Comparison of the ALE-FEM results and those of numerical method

Beam size(length×width×height) μm³	Gap(g) μm	β_{PI} ($\alpha=\eta=0$) Numerical	β_{PI} ($\alpha=\eta=0$) ALE
300×0.5×1	2.5	1.191	1.191
30×2.5×1	2.5	1.21	1.312
10×2.5×1	2.5	1.954	3.843

The comparison between ALE and Lagrangian methods is presented in Table 4. Note that while the ALE initial mesh is uniform, the initial Lagrangian mesh is denser in the beam root. However, as seen in Table 4, ALE method presents reliable results with fewer elements. Note that an arbitrary initially-selected Lagrangian mesh with denser mesh at the root might not be appropriate and optimization of the initial mesh to achieve an appropriate pattern might require further time-consuming analyses.

Table 4. Comparison of the ALE results and Lagrangian method in the case of Lagrangian FEM,
denser mesh has been applied in beam root where the length of elements at root is
1/3 of tip elements. Uniform mesh is applied for ALE analysis

Number of elements (horizontal element × vertical element)	With Casimir effects(β_{PI}) Lagrangian	With Casimir effects(β_{PI}) ALE	With van der Waals effects(β_{PI}) Lagrangian	With van der Waals effects(β_{PI}) ALE
20×4	0.7171	0.8181	0.5765	0.6677
50×4	0.8178	0.8191	0.6675	0.6686

Note that, while the benefits of using ALE-FEM (instead of other Lagrangian-FEM) might not be surprising in simple NEMS problems, this could effectively reduce the computational cost in complex cases, e.g. damage and plastic deformation of dynamic NEMS, etc.

4. CONCLUSION

In this article, an ALE-FEM was applied to investigate the static instability of cantilever beam-type nano-actuators. The influence of electrostatic field (Coulomb force) and quantum vacuum fluctuations (Casimir attraction and van der Waals force) were incorporated in the model. It was shown that the fringing field increased the pull-in deflection while decreasing the pull-in voltage of the system. On the other hand, quantum vacuum fluctuations decreased both instability parameters of the system. The obtained results were compared with those of numerical and analytical methods reported in the literature. The comparison revealed that ALE-FEM could be applied as a reliable approach for simulating the pull-in instability of cantilever nano-actuators and designing nano-electromechanical systems.

REFERENCES

1. Reddy, J. N. (2004). *An introduction to nonlinear finite element analysis.* Oxford University Press.
2. Gadala, M. S. (2004). Recent trends in ALE formulation and its applications in solid mechanics. *Comput. Meth. Appl. Mech. Eng.*, Vol. 193, pp. 4247-4275.
3. Tadi beni, Y., Movahhedy, M. R. & Farrahi, G. H. (2009). Rate dependent dynamic ALE analysis of finite deformation of elasto-viscoplastic solids. *Materials and Design*, Vol. 30, No. 8, pp. 2995-3004.
4. Tadi beni, Y. & Movahhedy, M. R. (2010). Consistent arbitrary Lagrangian Eulerian formulation for large deformation thermo-mechanical analysis. *Materials and Design*, Vol. 31, No. 8, pp. 3690-3702.
5. Tadi beni, Y., Movahhedy, M. R. & Farrahi, G. H. (2010). A complete treatment of thermo-mechanical ALE analysis; Part I: Formulation. *Iranian journal of Science & Technology, Transaction B, Engineering*, Vol. 34, No. B2, pp. 135-148.
6. Tadi beni, Y., Movahhedy, M. R. & Farrahi, G. H. (2010). A complete treatment of thermo-mechanical ALE analysis; Part 2: Finite element equations and applications. *Iranian Journal of Science & Technology, Transaction B, Engineering*, Vol. 34, No. B2, pp. 149-165.
7. Moghimi Zand, M. & Ahmadian, M. T. (2007). Characterization of coupled-domain multi-layer microplates in pull-in phenomenon, vibrations and dynamics. *Int. J. Mech. Sci.*, Vol. 49, No. 11, pp. 1226-1237.
8. Collenz, A., De Bona, F., Gugliotta, A. & Soma, A. (2004). Large deflections of microbeams under electrostatic loads. *J. Micromech. Microeng.*, Vol. 14, pp. 365–73.
9. Das, K, & Batra, R. C. (2009). Pull-in and snap-through instabilities in transient deformations of microelectromechanical systems. *J. Micromech. Microeng.*, Vol. 19, 035008 (19pp).
10. Brusa, E. & Munteanu, M. G. (2006). Coupled-field FEM nonlinear dynamics analysis of continuous Microsystems by non-incremental approach Analog Integr. *Circuits Signal Process.*, Vol. 48, pp. 7–14.
11. Pamidighantam, S., Puers, R., Baert, K. & Tilmans, H.A.C. (2002). Pull-in voltage analysis of electrostatically actuated beam structures with fixed–fixed and fixed-free end conditions. *J. Micromech. Microeng.* Vol. 12, pp. 458–64.
12. Buks, E. & Roukes, M. L. (2001). Metastability and the Casimir effect in micromechanical systems. *Europhys. Lett.*, Vol. 54, No. 2, p. 220.
13. Lamoreaux, S. K. (2005). The Casimir force: background, experiments, and applications. *Rep. Prog. Phys.* Vol. 68, pp. 201–36.
14. Buks, E. & Roukes, M. L. (2001). Stiction, adhesion energy, and the Casimir effect in micromechanical systems, *Phys. Rev. B*, Vol. 63, 033402.
15. Lin, W. H. & Zhao, Y. P. (2005). Casimir effect on the pull-in parameters of nanometer switches. *Microsyst. Techno.*, Vol. 11, pp. 80-85.
16. Lin, W. H. & Zhao, Y. P. (2005). Nonlinear behavior for nanoscale electrostatic actuators with Casimir force, *Chaos Solitons Fractals*, Vol. 23, pp. 1777–1785.

17. Abadyan, M., Novinzadeh, A. & Kazemi, A. S. (2010). Approximating the effect of the Casimir force on the instability of electrostatic nano-cantilevers. *Phys. Scr*. Vol. 81, 015801(10pp).

18. Ma, J. B., Jiang, L. & Asokanthan, S. F. (2010). Influence of surface effects on the pull-in instability of NEMS electrostatic switches. *Nanotechnology*, Vol. 21, 505708.

19. Koochi, A., Kazemi, A. S., Tadi Beni, Y., Yekrangi, A. & Abadyan, M. (2010). Theoretical study of the effect of Casimir attraction on the pull-in behavior of beam-type NEMS using modified Adomian method. Physica E, Vol. 43, pp. 625–632.

20. Batra, R. C., Porfir, M. & Spinello, D. (2008). Reduced-order models for microelectromechanical rectangular and circular plates incorporating the Casimir force. *Int. J. Solids Struct*., Vol. 45, pp. 3558–3583.

21. Batra, R. C., Porfiri, M. & Spinello, D. (2008). Vibrations and pull-in instabilities of microelectromechanical von Karman elliptic plates incorporating the Casimir force. *J. of Sound and Vibration*, Vol. 315, pp. 939–960.

22. Moghimi Zand, M., Ahmadian, M. T. & Rashidian, B. (2010). Dynamic pull-in instability of electrostatically actuated beams incorporating Casimir and van der Waals forces. *Proc. Inst. Mech. Eng. Part C*, Vol. 224, No. 9, p. 2037.

23. Gupta, R. K. (1997). Electrostatic pull-in test structure design for in-situ mechanical property measurements of microelectromechanical systems. PhD Dissertation Massachusetts Institute of Technology (MIT), Cambridge, MA.

24. Israelachvili, J. N. & Tabor, D. (1972). Measurement of Van der Waals dispersion forces in range 1.5 to 130 nm. *Proc. Roy. Soc. Lond. A*, 331(1584): 19.

25. Gadala, M. S., Movahhedy, M. R. & Wang, J. (2002). On the mesh motion for ALE modeling of metal forming processes. *Finite Elements in Analysis and Design*, Vol. 38, pp. 435-459.